Сверхсветовые Нейтрино

Ю.Н.Гнедин, ГАО РАН

Нейтринный эксперимент CNGS:

CERN Neutrino beam to Gran Sacco – 730 km

$$p \to \mu^{\pm} + \nu_{\mu}; \qquad \frac{v-c}{c} = \left(2.48 \pm 0.28\left(stat\right) + 0.3\left(syst\right)\right) \times 10^{-5}$$

Три семейства фундаментальных частиц

Семейство 1

Электрон $m_e = 0,00054 m_p$

Электронное нейтрино $m_{\nu_e} < 10^{-8} m_p$

U–кварк $0,047 m_p$

d-кварк $0,0074 m_p$

Семейство 2

Мюон $m_\mu = 0,11 m_p$

Мюоное нейтрино $m_{\nu_\mu} < 0,0003 m_p$

C-кварк $1,6 m_p$

S-кварк $0,16 m_p$

Семейство 3

Тау-мезон $m_\tau = 1,9 m_p$

Тау-нейтрино $m_{\nu_\tau} < 0,033 m_p$

t-кварк $189,0 m_p$

b-кварк $5,2 m_p$

An appearance experiment to search for $\nu_\mu \leftrightarrow \nu_\tau$ oscillations in the CNGS beam

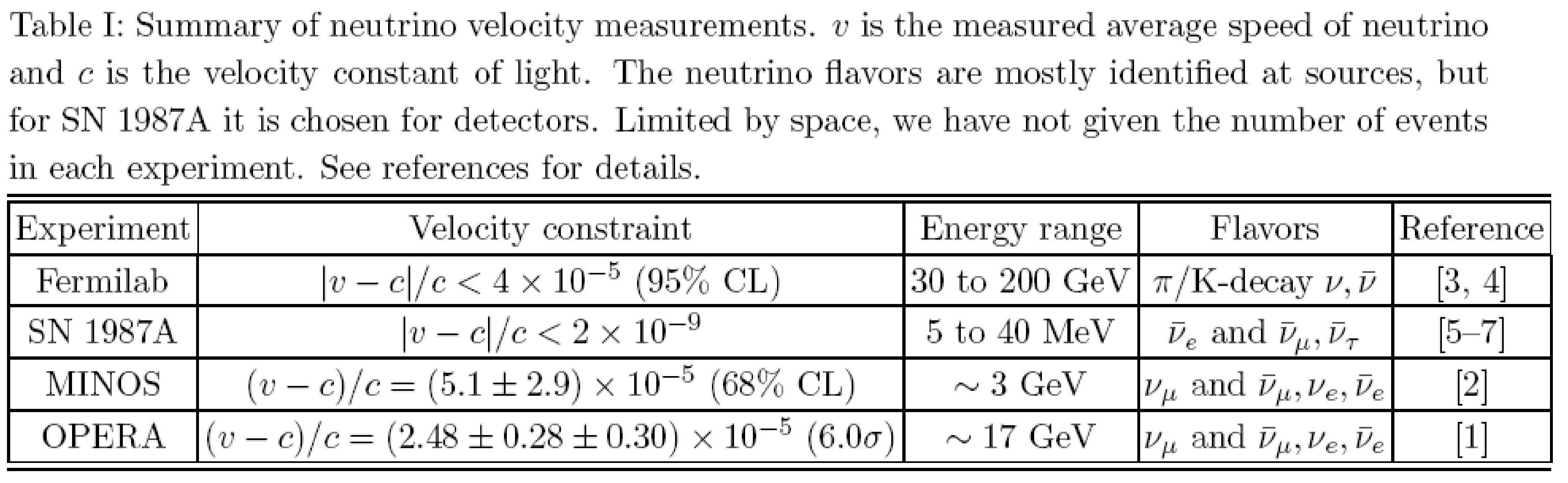

Table I: Summary of neutrino velocity measurements. v is the measured average speed of neutrino and c is the velocity constant of light. The neutrino flavors are mostly identified at sources, but for SN 1987A it is chosen for detectors. Limited by space, we have not given the number of events in each experiment. See references for details.

Experiment	Velocity constraint	Energy range	Flavors	Reference
Fermilab	$\lvert v - c \rvert / c < 4 \times 10^{-5}$ (95% CL)	30 to 200 GeV	π/K-decay $\nu, \bar{\nu}$	[3, 4]
SN 1987A	$\lvert v - c \rvert / c < 2 \times 10^{-9}$	5 to 40 MeV	$\bar{\nu}_e$ and $\bar{\nu}_\mu, \bar{\nu}_\tau$	[5–7]
MINOS	$(v - c)/c = (5.1 \pm 2.9) \times 10^{-5}$ (68% CL)	~ 3 GeV	ν_μ and $\bar{\nu}_\mu, \nu_e, \bar{\nu}_e$	[2]
OPERA	$(v - c)/c = (2.48 \pm 0.28 \pm 0.30) \times 10^{-5}$ (6.0σ)	~ 17 GeV	ν_μ and $\bar{\nu}_\mu, \nu_e, \bar{\nu}_e$	[1]

Miao Li & Tower Wang arXiv:1109.5924

T. Adam et al. arXiv:1109.4897

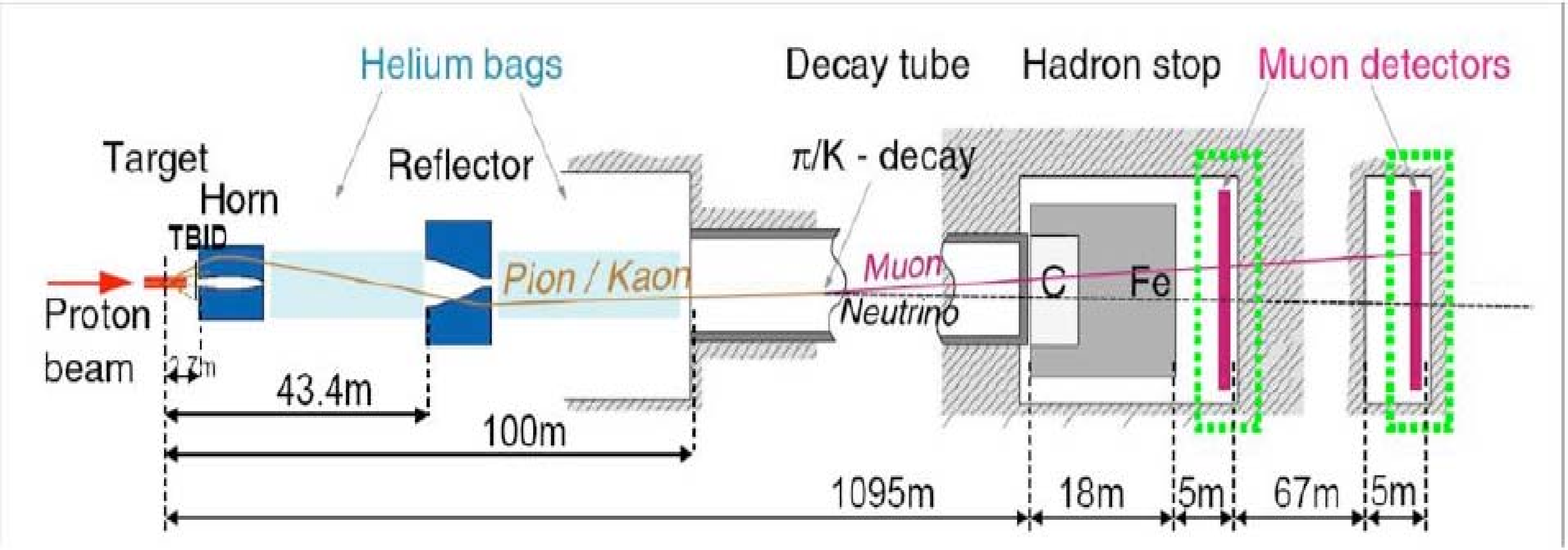

Fig.2: Layout of the CNGS beam line.

T. Adam et al. arXiv:1109.4897

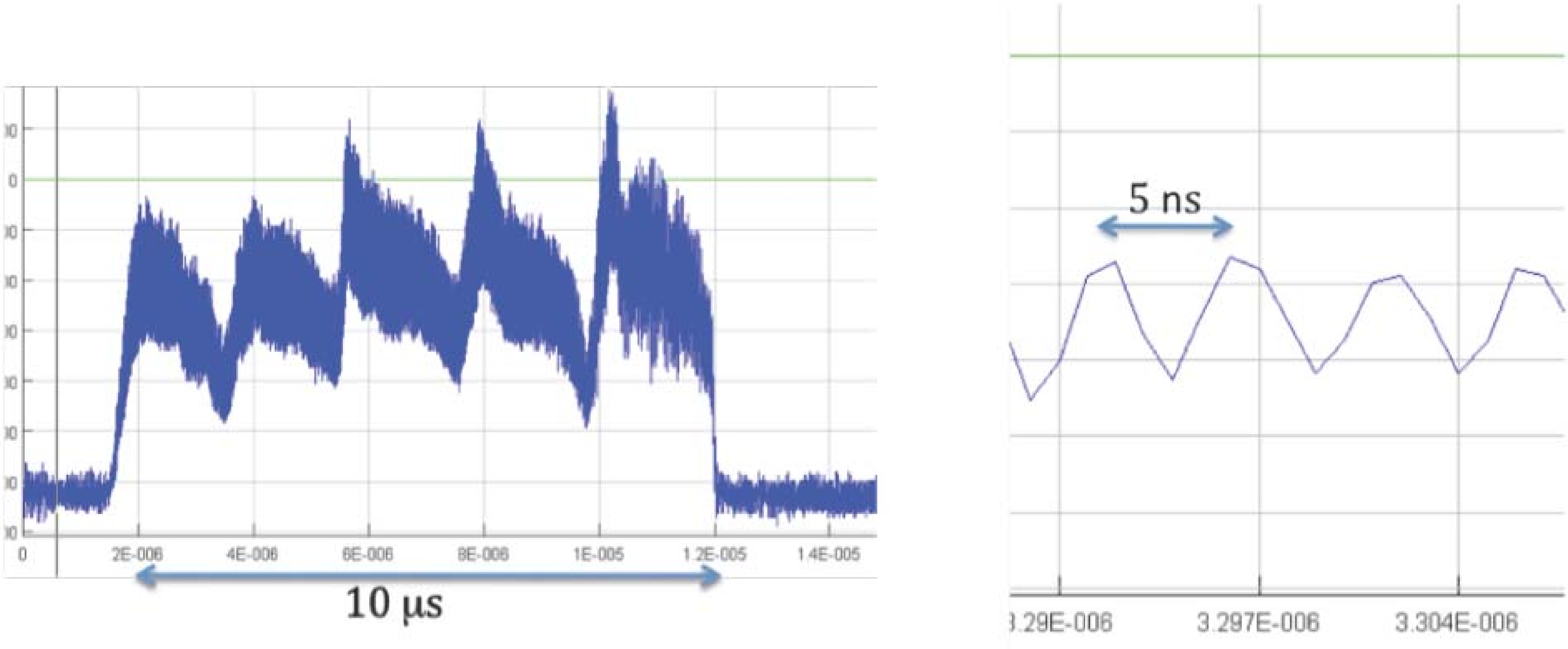

Fig. 4: Example of a proton extraction waveform measured with the BCT detector BFCTI400344. The five-peak structure reflects the continuous PS turn extraction mechanism. A zoom of the waveform (right plot) allows resolving the 200 MHz SPS radiofrequency.

T. Adam et al. arXiv:1109.4897

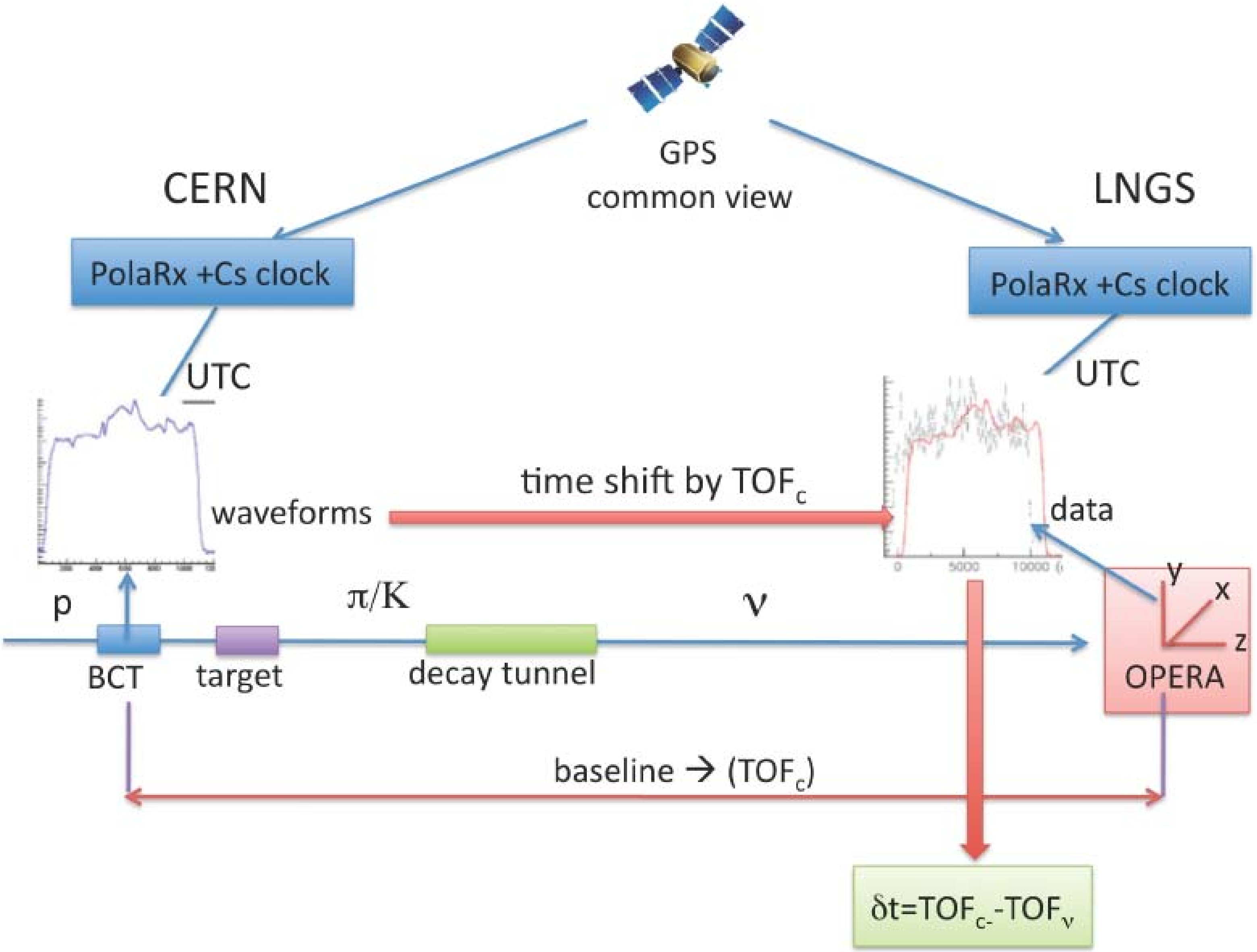

Fig. 5: Schematic of the time of flight measurement.

T. Adam et al. arXiv:1109.4897

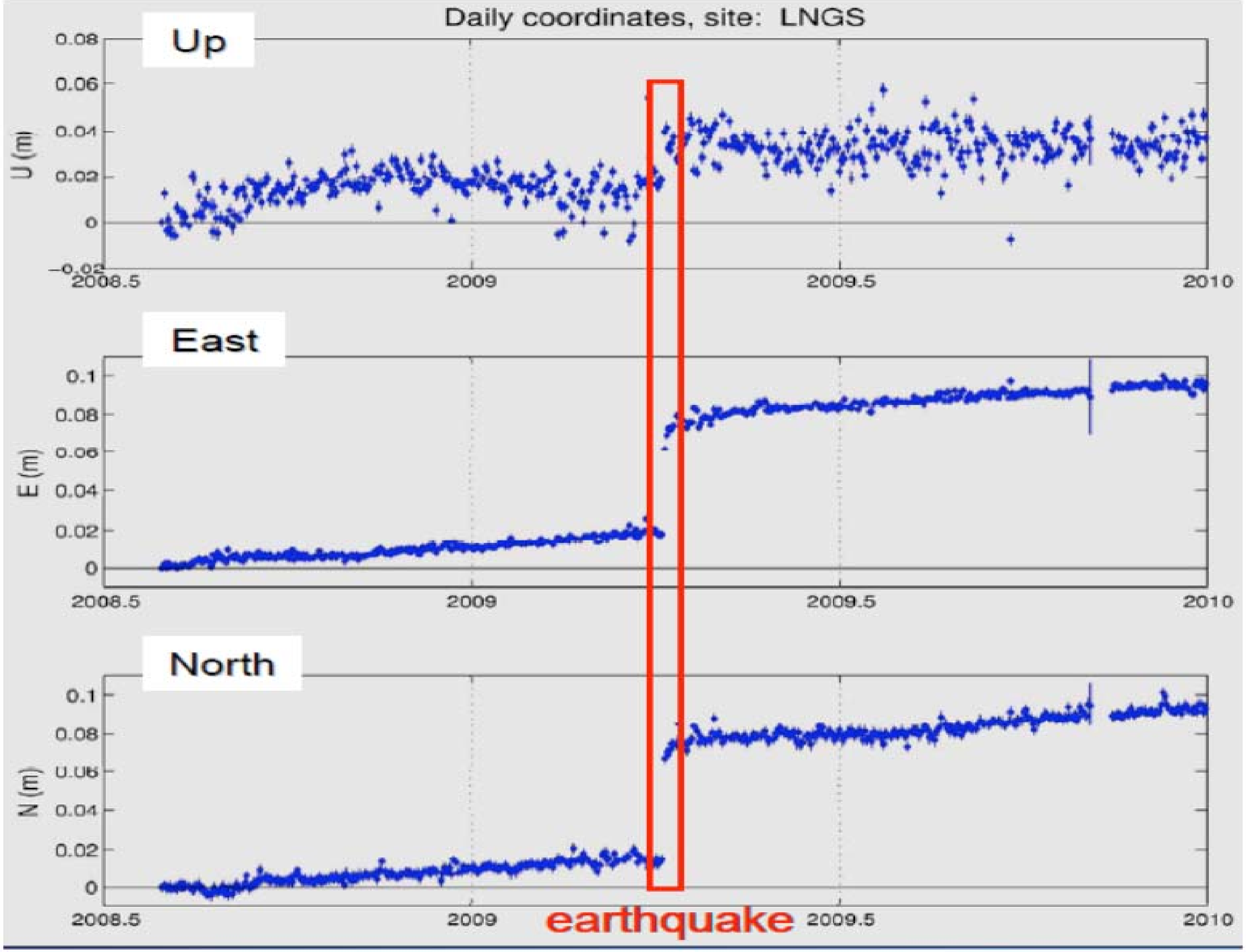

Fig. 7: Monitoring of the PolaRx2e GPS antenna position at LNGS, showing the slow earth crust drift and the fault displacement due to the 2009 earthquake in the L'Aquila region. Units for the horizontal (vertical) axis are years (meters).

T. Adam et al. arXiv:1109.4897

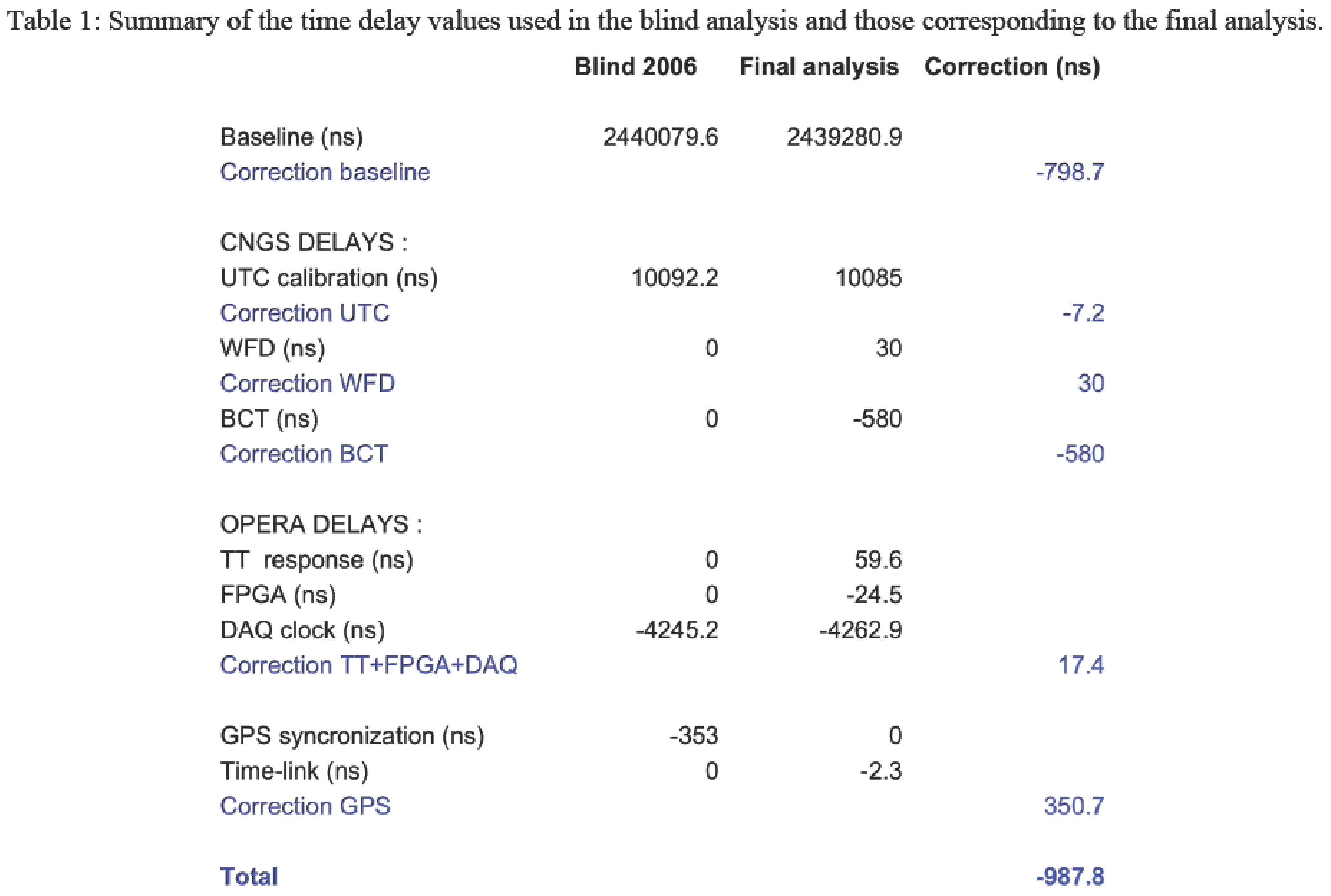

Table 1: Summary of the time delay values used in the blind analysis and those corresponding to the final analysis.

	Blind 2006	Final analysis	Correction (ns)
Baseline (ns)	2440079.6	2439280.9	
Correction baseline			-798.7
CNGS DELAYS :			
UTC calibration (ns)	10092.2	10085	
Correction UTC			-7.2
WFD (ns)	0	30	
Correction WFD			30
BCT (ns)	0	-580	
Correction BCT			-580
OPERA DELAYS :			
TT response (ns)	0	59.6	
FPGA (ns)	0	-24.5	
DAQ clock (ns)	-4245.2	-4262.9	
Correction TT+FPGA+DAQ			17.4
GPS syncronization (ns)	-353	0	
Time-link (ns)	0	-2.3	
Correction GPS			350.7
Total			**-987.8**

T. Adam et al. arXiv:1109.4897

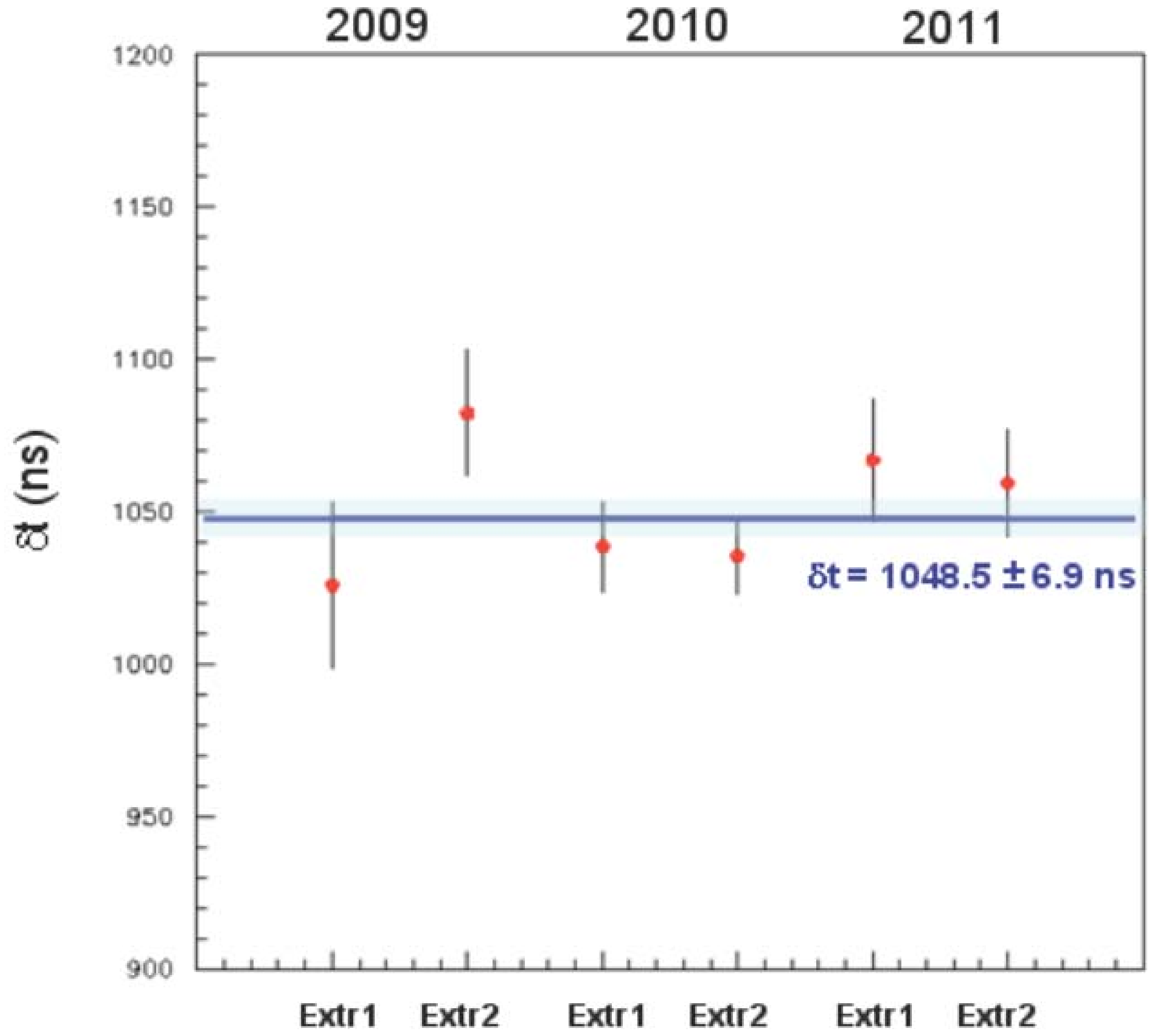

Fig. 10: Results of the maximum likelihood analysis for δt corresponding to the two SPS extractions for the 2009, 2010 and 2011 data samples.

T. Adam et al. arXiv:1109.4897

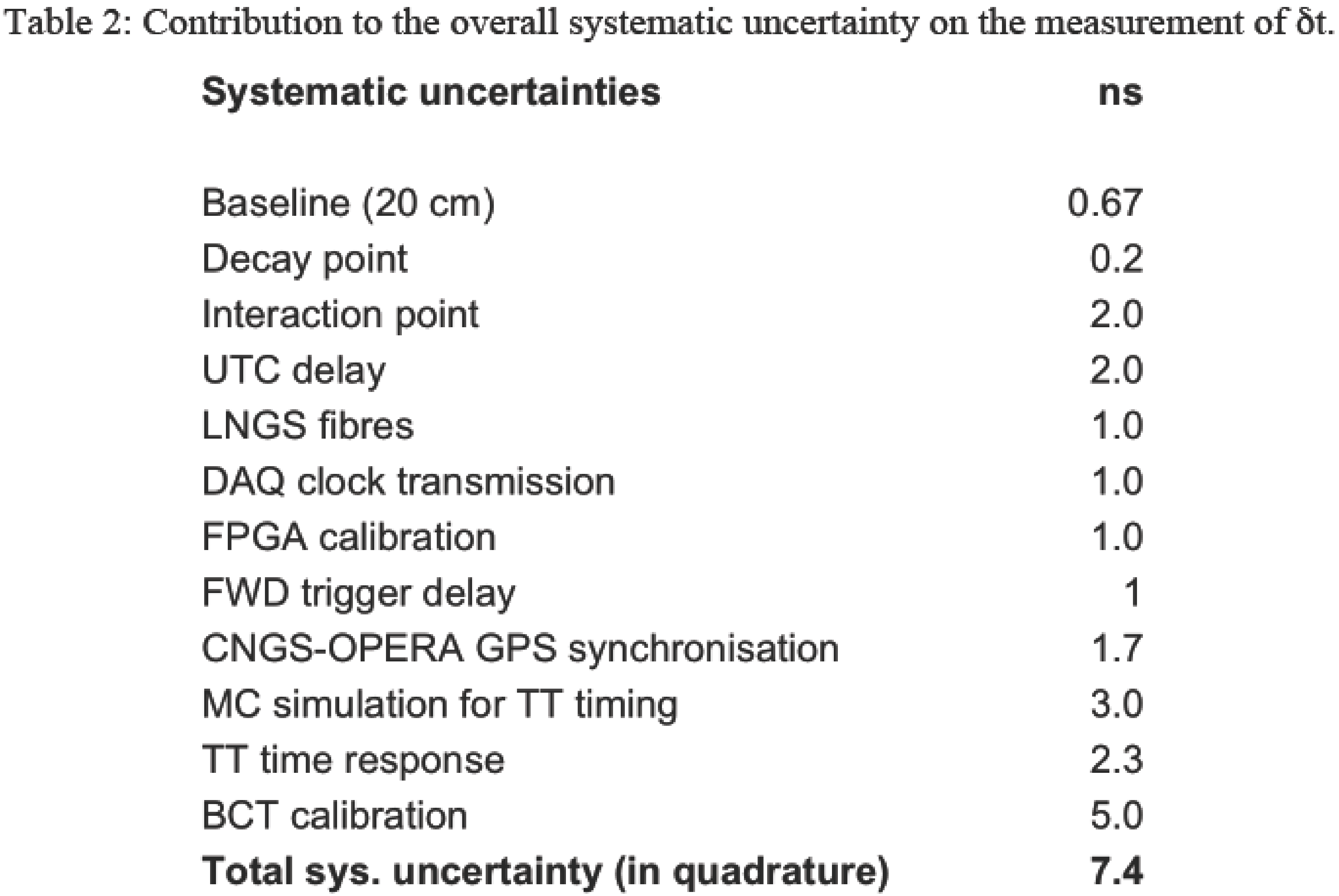

Table 2: Contribution to the overall systematic uncertainty on the measurement of δt.

Systematic uncertainties	**ns**
Baseline (20 cm)	0.67
Decay point	0.2
Interaction point	2.0
UTC delay	2.0
LNGS fibres	1.0
DAQ clock transmission	1.0
FPGA calibration	1.0
FWD trigger delay	1
CNGS-OPERA GPS synchronisation	1.7
MC simulation for TT timing	3.0
TT time response	2.3
BCT calibration	5.0
Total sys. uncertainty (in quadrature)	**7.4**

T. Adam et al. arXiv:1109.4897

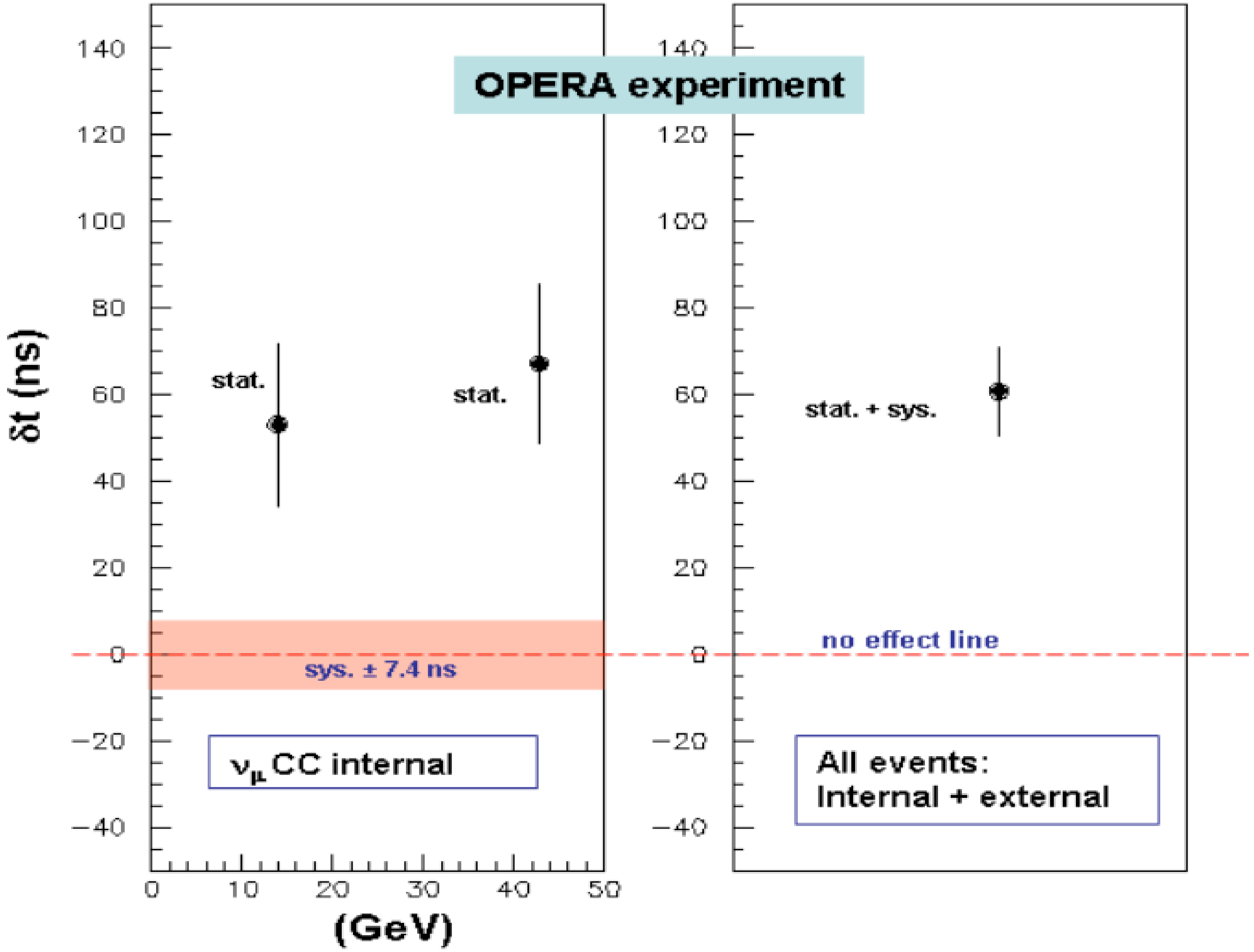

Fig. 13: Summary of the results for the measurement of δt. The left plot shows δt as a function of the energy for ν_μ CC internal events. The errors attributed to the two points are just statistical in order to make their relative comparison easier since the systematic error (represented by a band around the no-effect line) cancels out. The right plot shows the global result of the analysis including both internal and external events (for the latter the energy cannot be measured). The error bar includes statistical and systematic uncertainties added in quadrature.

T. Adam et al. arXiv:1109.4897

Нарушение принципа Лоренцевой симметрии

Классическая теория Эйнштейна:

$$1-\frac{v^2}{c^2}=\frac{m^2c^4}{E^2}$$

Нарушение Лоренц-симметрии:

$$1-\frac{v^2}{c^2}=\lambda-f\left(\lambda\right):\ \lambda=\frac{m^2c^4}{E^2}$$

Критическая энергия нарушения симметрии Лоренца:

$$E_{\text{кр}}=\frac{mc^2}{\sqrt{\lambda_{\text{кр}}}}$$